# A Possible Evolutionary Channel for the Recently Discovered Class of Millisecond Pulsars in Long, Eccentric Orbits

Undergraduate Research Thesis

Presented in Partial Fulfillment of the Requirements for graduation "with Honors Research Distinction in Astronomy" in the undergraduate colleges of The Ohio State University

by
Andrew Taylor

The Ohio State University
October 2017

Project Advisor: Professor Todd Thompson, Department of Astronomy

# A Possible Evolutionary Channel for the Recently Discovered Class of Millisecond Pulsars in Long, Eccentric Orbits

Andrew J. Taylor
The Ohio State University

October 18, 2017

**Abstract**

We consider an evolutionary channel for the recently discovered class of millisecond pulsars (MSPs) on relatively long, eccentric binary orbits. If the standard model for formation of MSPs involving a low-mass X-ray binary (LMXB) mass transfer stage is the origin of these systems, the observed companion cannot have been the star involved in the binary interaction with the pulsar. Instead, we consider a tight triple system, where the nearby binary companion is ablated away, as in observed black widow and redback systems. The tertiary induces Kozai-Lidov eccentricity oscillations, enhancing mass loss. We solve the secular equations for triple dynamics including ablative mass loss. We demonstrate that eccentricity-aided ablation reduces the timescale required for the MSP to ablate its companion by a modest factor and increases the parameter space of initial systems that may lead to what we observe today. We find that the approximate dependence of the overall timescale for ablation on eccentricity is $(1 - e_{1,max})^{1/15}$, assuming low initial eccentricity, where $e_{1,max}$ is the maximum eccentricity of the inner binary driven by Kozai-Lidov oscillations. We survey the parameter space of binaries using a public Binary Stellar Evolution code. Next, we inject tertiaries with randomly chosen orbital parameters to search for systems satisfying the "outer" semimajor axes we observe today. We find no surviving systems with outer semimajor axis less than 1 AU, in conflict with the observations, and suggesting binary and triple star evolution not captured by the standard theory. We point to triple common envelope evolution as a possible formation method for tight, stable triple systems. We conclude that eccentricity-aided ablation is capable of reducing the ablation timescale of dynamically active triple systems by modest factors, and this works to increase the number of systems that can produce long-orbit, eccentric MSP systems.

## 1 Introduction

The recent discovery of a class of Millisecond Pulsars (MSPs) in relatively long, eccentric binary orbits raises questions about the formation of these systems. The accepted model for the formation of MSPs is through "recycling", whereby a nearby binary companion star overflows its Roche lobe and transfers mass to the neutron star (NS) primary, increasing its rate of rotation and partially burying its strong magnetic field (Alpar et al., 1982). Such systems are referred to as recycled MSPs, as their spin period is in the millisecond range. These pulsars have relatively low magnetic field strengths ($B \sim 10^9$ G) with spindown timescales of $10^8$ years. For more discussion of MSP formation and the observed population, see Özel & Freire (2016) and references therein. The recycling formation process requires orbital periods of a few days at most, and tidal forces, as well as common envelope (CE) evolution, would have circularized these tight orbits. Therefore, it was surprising when systems were discovered with eccentricity $0.027 < e < 0.44$ and periods from 22 - 95 days (Champion et al., 2008; DeCesar et al., 2015; Antoniadis et al., 2016; Barr

et al., 2017; Knispel et al., 2015). These isolated MSPs are a new type of system, so they require a new formation channel.

Regarding the system PSR J1903+0327 (Champion et al., 2008), Freire et al. (2011) proposed a tight triple system that then evolved into a binary, suggesting its current companion is not the star that recycled it; Pijloo et al. (2012) explored tertiary-induced dynamical ejection of the secondary as a possible evolutionary channel for producing such systems. In this paper, we explore how three-body dynamics may lead to the systems we observe. We explore the concept of eccentricity-aided ablation and its potential to eliminate the secondary from a hierarchical triple system, leaving the primary and tertiary behind as the binary we observe today. We present numerical calculations of the evolution of sample triple systems and report the outcomes of the systems. In section 2, we explore the concept of eccentricity-aided ablation. In section 3, we consider the effects of eccentricity-aided ablation on a theoretical tight MSP binary with a hierarchical tertiary. In section 4, we discuss possible original triple systems that lead to what we observe today. In section 5, we discuss possible future directions for this project and areas left unexplored. Finally, in section 6, we present our conclusions and discuss the implications of our findings.

# 2 Evolutionary Equations for Triple Systems with Ablative Mass Loss

## 2.1 The Eccentric Kozai Mechanism

Lidov (1962) and Kozai (1962) demonstrated that in hierarchical triple systems with high mutual inclination between the inner and outer orbits, the inner binary can be driven to high eccentricity. Assuming a test-particle mass secondary, to quadrupole order in the perturbing Hamiltonian, the maximum possible eccentricity attainable by the inner binary becomes (Lidov, 1962; Kozai, 1962)

$$e_{1,max} = \left(1 - \frac{5}{3}\cos^2(i)\right)^{1/2}. \tag{1}$$

This expression applies for $|\cos(i)| < \sqrt{3/5}$ ($39^\circ < i < 141^\circ$), where $i$ is the mutual inclination between the inner and outer orbits, and the timescale in between oscillations is given by Innanen et al. (1997) as

$$\begin{aligned}\tau_{KL} &\sim \frac{P_{out}^2}{P_{in}}(1-e_2^2)^{3/2} \\ &= 77 \text{ yr} \left(\frac{a_1}{0.1 \text{ AU}}\right)^{3/2} \left(\frac{m_0+m_1}{2M_\odot}\right)^{1/2} \left(\frac{m_2}{M_\odot}\right)^{-1} \left(\frac{a_2/a_1}{20}\right)^{3} (1-e_2^2)^{3/2},\end{aligned} \tag{2}$$

where $P_{out}$ and $P_{in}$ are the periods of the outer and inner binary orbits, $a_2$ and $a_1$ are the semimajor axes of the outer and inner binary orbits, $m_0, m_1$, and $m_2$ are the masses of the primary, secondary, and tertiary, and $e_2$ is the eccentricity of the outer binary orbit.

Lidov and Kozai were interested in the perturbations of the Sun and Jupiter on asteroids and artificial satellites. The Kozai-Lidov (KL) mechanism was next applied as an explanation for close stellar binary systems (Mazeh & Shaham, 1979) and to the existence of so-called "Hot Jupiters" (Wu & Murray, 2003; Fabrycky & Tremaine, 2007). Blaes et al. (2002), Miller & Hamilton (2002), and Wen (2003) took this another step further, showing that the KL mechanism can significantly decrease the merger time of a compact object binary system due to gravitational wave (GW) emission. Thompson (2011) argued that the KL mechanism may be largely responsible for the rate of type Ia supernovae (SNe) via white dwarf-white dwarf (WD-WD) mergers, and several groups have recently argued that the black hole-black hole (BH-BH) merger rate may be dominated by KL-stimulated GW emission (Silsbee & Tremaine, 2017; Antonini et al., 2017).

Katz et al. (2011) and Lithwick & Naoz (2011) introduced the parameter $\epsilon_{oct}$, which describes the strength of the octupole-order terms in the perturbing three-body Hamiltonian, which can cause orbital flips, driving the inclination from prograde to retrograde, and very high $e_1$. To a higher order in $a_1/a_2$ than evaluated in Equation 1, slightly retrograde tertiaries produce higher maximum eccentricities in inner binaries than prograde ones. Naoz et al. (2013) added a term onto the $\epsilon_{oct}$ of Katz et al. (2011) and Lithwick & Naoz (2011) that depends on the difference in masses between the primary and secondary, and we adopt that here as well. We define $\epsilon_{oct}$ as:

$$\epsilon_{oct} = \left(\frac{m_0 - m_1}{m_0 + m_1}\right)\left(\frac{a_1}{a_2}\right)\frac{e_2}{1 - e_2^2} \tag{3}$$

where $a_2$ and $e_2$ are the semimajor axis and eccentricity of the outer orbit. For $m_0 \sim m_1$, the octupole terms have little strength, and we say that the Eccentric Kozai Mechanism is "turned off." However, for $m_1 \ll m_0$, the inner binary can be driven to much higher eccentricities ($1 - e_1 \sim 10^{-6}$) than the quadrupole terms alone can achieve. For example, Shappee & Thompson (2013) showed that even initially equal-mass binaries can undergo extreme eccentricity oscillations after one of the bodies undergoes significant mass loss as it evolves to a compact object (see discussion of Figure 1 below).

## 2.2 Adiabatic Mass Loss

Ford et al. (2000) and Blaes et al. (2002) solved the three-body Hamiltonian to octupole order in the limit of a hierarchical triple (small $a_1/a_2$), using orbit-averaging to arrive at a system of ordinary differential equations (ODEs) for the system's dynamics. Michaely & Perets (2014) added terms to these equations to account for the effects of adiabatic mass-loss (their Equations 50 and 51). We re-write them here for clarity (assuming the companion $m_1$ is losing mass at a rate of $\dot{m}_1 > 0$):

$$\dot{a}_1 = \frac{\dot{m}_1}{m_0 + m_1} a_1 \tag{4}$$

$$\dot{a}_2 = \frac{\dot{m}_1}{m_0 + m_1 + m_2} a_2. \tag{5}$$

Because $a_1$ and $a_2$ change as a result of mass loss, so too do the angular momenta of the inner and outer binaries. Defining the angular momenta $G_1$ and $G_2$ as

$$G_1 = m_0 m_1 \left(\frac{G a_1 (1 - e_1^2)}{m_0 + m_1}\right)^{1/2} \tag{6}$$

$$G_2 = (m_0 + m_1) m_2 \left(\frac{G a_2 (1 - e_2^2)}{m_0 + m_1 + m_2}\right)^{1/2}, \tag{7}$$

it follows that the rate of change of $G_1$ and $G_2$ is

$$\dot{G}_{1,ML} = \frac{m_0 \dot{m}_1}{m_1 (m_0 + m_1)} G_1 \tag{8}$$

$$\dot{G}_{2,ML} = \frac{m_2 \dot{m}_1}{(m_0 + m_1)(m_0 + m_1 + m_2)} G_2. \tag{9}$$

Note that the angular momentum per unit mass is conserved. Thus, at the test particle limit, the entire angular momentum would be conserved. To find the rate of change of the total angular momentum, $H$, we use the definition of $H$ in terms of $G_1$ and $G_2$, as well as the relation that

$$G_1 \cos(i_1) = \frac{H^2 + G_1^2 - G_2^2}{2H} \tag{10}$$

$$G_2 \cos(i_2) = \frac{H^2 - G_1^2 + G_2^2}{2H}, \tag{11}$$

we arrive at

$$\begin{aligned}\dot{H}_{ML} &= \frac{d}{dt}(G_1\cos(i_1) + G_2\cos(i_2)) \\ &= \dot{G}_1\cos(i_1) + \dot{G}_2\cos(i_2) \\ &= \frac{\dot{m}_1}{2H(m_0+m_1)}\left(\frac{m_0}{m_1}(H^2+G_1^2-G2^2) + \frac{m_2}{m_0+m_1+m_2}(H^2-G_1^2+G_2^2)\right). \end{aligned} \quad (12)$$

The other orbital elements used in the Ford et al. (2000) and Blaes et al. (2002) equations ($e_1$, $g_1$, $e_2$, and $g_2$) are unchanged by adiabatic mass loss.

We combined these equations with those in Ford et al. (2000) and Blaes et al. (2002) to arrive at a system of equations for the secular evolution of a binary system undergoing adiabatic mass loss, GW radiation, and GR precession. The equations are solved using two integrators: one in Python and one in C++. Both methods were able to produce Figure 1. The method used in the process of determining the eccentric mass-loss factor (EMLF–described in more detail in Section 2.3) is the odeint integrator from Python's scipy.integrate. The integrator uses lsoda from the FORTRAN library odepack and solves first-order ODEs through numerical integration. The method used for the integration of orbital elements of systems (described in more detail in Section 3) is an integrator in the odeint package from boost in C++. Specifically, the integrator is a 5th order Runge-Kutta integrator with 4th order error estimation and coefficients introduced by Cash & Karp (1990). In Figure 1, we present a reproduction of Figure 4 from Michaely & Perets (2014) with our code, as a verification of our equations and integrator. The upper left panel demonstrates that the system had little excitation of the eccentricity until the primary began losing mass. This agrees with the argument of Shappee & Thompson (2013) that initially equal-mass binaries can experience extreme eccentricity oscillations after one of the bodies undergoes significant mass loss.

## 2.3 Ablation

MSPs emit a highly energetic wind, and many believe it is possible for a pulsar to ablate its companion (so-called "redback" and "black-widow" pulsars, e.g., King et al. 2003, Phinney et al. 1988). We consider the possibility of a binary composed of a MSP and a main sequence (MS) star in a hierarchical triple system, tight enough for the MSP to significantly ablate away its companion. The inner binary would be driven to very high eccentricities by the KL mechanism; because the relative difference in mass between the MSP primary and the MS secondary is so great (see Özel & Freire (2016) and references therein for an estimate of the average mass of MSP companions), $\epsilon_{oct}$ is high, so the binary could be driven to high eccentricity. As the eccentricity increases, the periastron distance decreases, and we expect the rate of ablative mass-loss averaged over a period to increase.

van den Heuvel & van Paradijs (1988) use energy conservation to derive an expression for the mass-loss rate $\dot{M}$ of the companion star of an ablator in the case of a circular orbit. They begin with the rate of energy loss of the pulsar

$$\dot{E}_{NS}^{wind} = \frac{2B^2\Omega^4R_0^6}{3c^3}, \quad (13)$$

where $B$, $R_0$, and $\Omega$ are the pulsar's magnetic field strength, radius, and spin frequency ($\Omega = 2\pi/P_{spin}$). Equating the fraction of the pulsar wind that intercepts the companion with the kinetic power of a steady wind reaching escape velocity,

$$\dot{E}_1^{escape} = \frac{1}{2}\dot{m}_1v_e^2 = \frac{Gm_1\dot{m}_1}{R_1}, \quad (14)$$

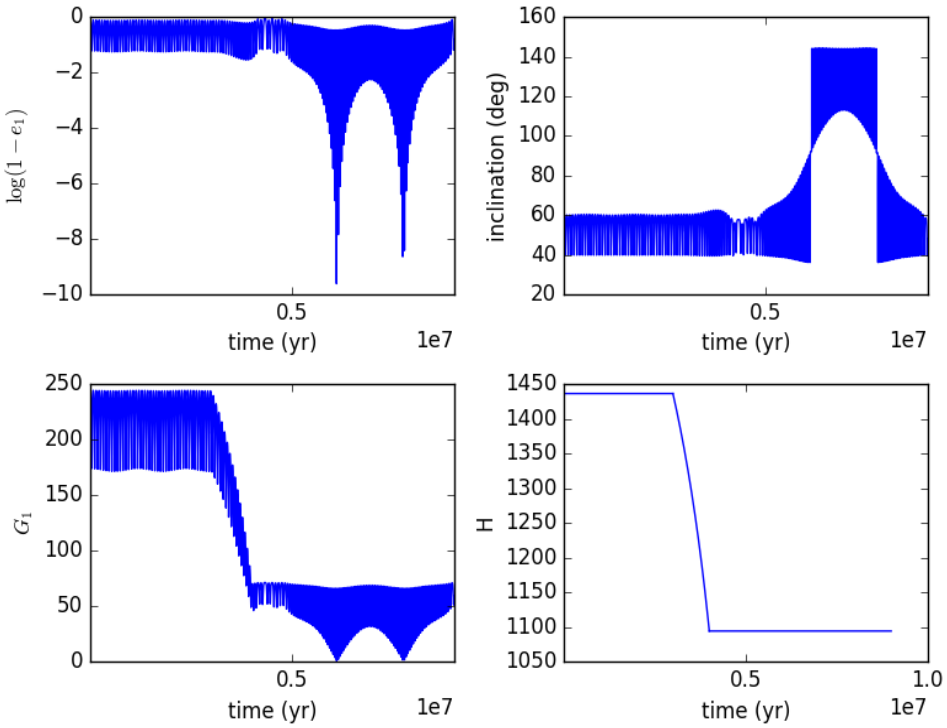


**Figure 1:** Evolution of a hierarchical triple, following Michaely & Perets (2014)(verifying the accuracy of our code). Initial conditions $m_0 = 7M_\odot$, $m_1 = 6.5M_\odot$, $m_2 = 6M_\odot$, $a_1 = 10$ AU, $a_2 = 250$ AU, $e_1 = 0.1$, $e_2 = 0.7$, $g_1 = 0$, $g_2 = 0$, $i = 60^\circ$. Constant mass-loss is introduced for $m_0$ at $t = 3$ Myr until $t = 4$ Myr and $m_0$ decreases to $1.15M_\odot$.

we find that

$$\dot{m}_{1,c} = \left(\frac{2R_0^6}{3c^3}\right)\left(\frac{R_1^3}{4a_1^2}\right)\left(\frac{B^2}{Gm_1}\right)\left(\frac{2\pi}{P}\right)^4 f$$
$$= 1.9\times10^{-9}M_\odot/\mathrm{yr}\left(\frac{R_1}{0.2R_\odot}\right)^3\left(\frac{a_1}{16R_\odot}\right)^{-2}\left(\frac{m_1}{0.2M_\odot}\right)^{-1}\left(\frac{P}{1.6\mathrm{ms}}\right)^{-4} f, \quad (15)$$

where $m_1$, $\dot{m}_{1,c}$, and $R_1$ are the companion mass, rate of mass-loss, and radius, respectively. Here we have assumed $R_0$ = 10 km and $B = 10^9$ G. van den Heuvel & van Paradijs (1988) argue that a fraction $(R_1/2a_1)^2$ of the energy emitted by the pulsar would actually make contact with the companion, as well as a second fraction, $f$, of the wind striking the companion that would actually drive mass to escape (although this may be of order unity). Here, we have assumed circular orbits.

We wish to generalize this expression to eccentric orbits by averaging $\dot{m}_1$. Averaging over orbital angle would lead to an overestimate of $\dot{m}_1$, as it fails to account for the relatively short amount of time spent at periastron (where ablation is strongest) and the relatively large amount of time spent at apastron (where ablation is weakest). In the limit of high eccentricity, all the mass-loss occurs at periastron. We can therefore make an order of magnitude estimate by setting the mass loss rate equal to

$$\dot{m}_1 \sim \frac{\dot{m}_{1,peri}\Delta t_{peri}}{P} \sim \frac{\dot{m}_{1,peri}\,(R_{peri}/v_{peri})}{P}. \quad (16)$$

Then, since $\dot{m}_{peri} \propto R_{peri}^{-2}$, writing this in terms of $e$, we find that

$$\dot{m}_1 \propto R_{peri}^{-2}\frac{R_{peri}}{v_{peri}} \propto (1-e_1)^{-2}\frac{(1-e_1)}{(1-e_1)^{-1/2}} = (1-e_1)^{-1/2}. \quad (17)$$

Therefore, for fixed orbital eccentricity, we expect an inverse square root relationship such that $\dot{m} \propto (1-e_1)^{-1/2}$, so that as $e_1 \rightarrow 1$, $\dot{m}_1 \rightarrow \infty$. The maximum $e_1$ is bounded by $R_1$, since for a tidally non-interacting system, $R_{peri} = a_1(1-e_1) < R_1$, which gives the maximum possible enhancement of $\dot{m}_1$ of $(1-e_{1,max})^{-1/2} = \sqrt{a_1/R_1}$ in Equation 15.

To make a complete calculation, numerically averaging over the orbit requires averaging the inverse square of the distance between the two bodies, $r = a_1(1-e_1 \cos E)$, where $E$ is the eccentric anomaly, over time for an orbital period. This requires solving the transcendental equation

$$E = M + e_1 \sin E \tag{18}$$

for many points in the orbit, where $M$ and $e_1$ are the mean anomaly and eccentricity. Averaging the inverse square of the distance over an orbit leads to the normalized integral

$$\xi(e_1) \equiv \left\langle \frac{a_1^2}{r^2} \right\rangle = \frac{1}{P}\int_0^P \frac{1}{(1-e_1 \cos E)^2} dt = \frac{1}{2\pi}\int_0^{2\pi} \frac{1}{(1-e_1 \cos E)^2} dM. \tag{19}$$

We define the function $\xi(e_1)$ as the normalized integral of the inverse square of the separation between two bodies in binary orbit. Figure 2 shows the integrand of Equation 19 for various values of $e_1$, and Figure 3 shows $\xi(e_1)$ as a function of eccentricity. Because a system undergoing KL oscillations can reach eccentricity up to $(1-e_1) \sim R_1/a_1 = 10^{-2.33}(R_1/R_\odot)(\mathrm{AU}/a_1)$, we show values spanning a wide range in $\log_{10}(1-e_1)$.

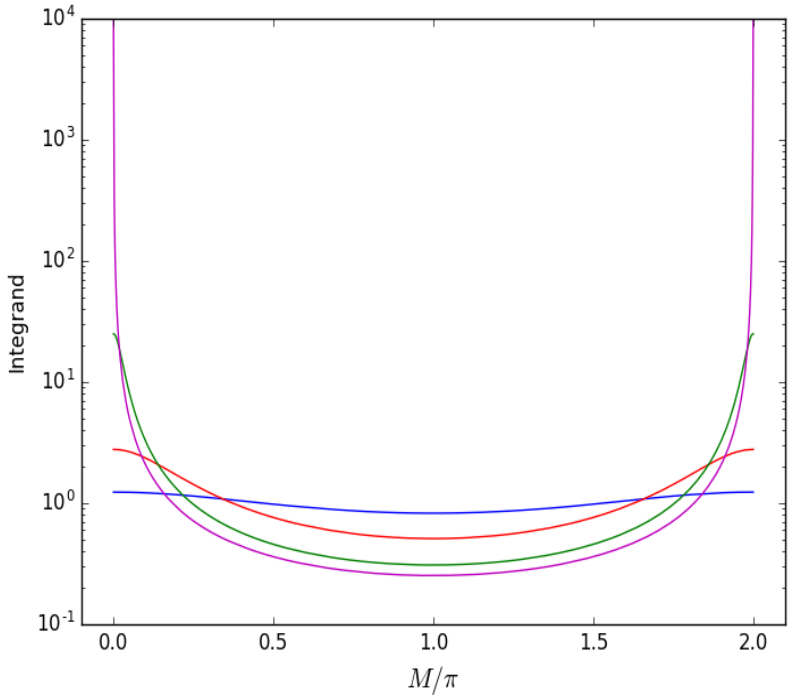


**Figure 2:** The integrand of Equation 19, $1/(1-e_1 \cos E)^2$, as a function of $M$ from 0 to $2\pi$, for $e_1$ = 0.1 (blue), 0.4 (red), 0.8 (green), and 0.99 (magenta). As $e_1$ approaches 1, the integrand becomes very large at periastron. As the orbit spends more and more of its time at apastron, all the mass loss should occur at periastron.

Figure 3 demonstrates that the mass-loss rate over a period can be increased by a factor of 1000 or more for eccentric systems as opposed to circular systems. We also show the relation $1/\sqrt{1-e_1}$ (red, solid)

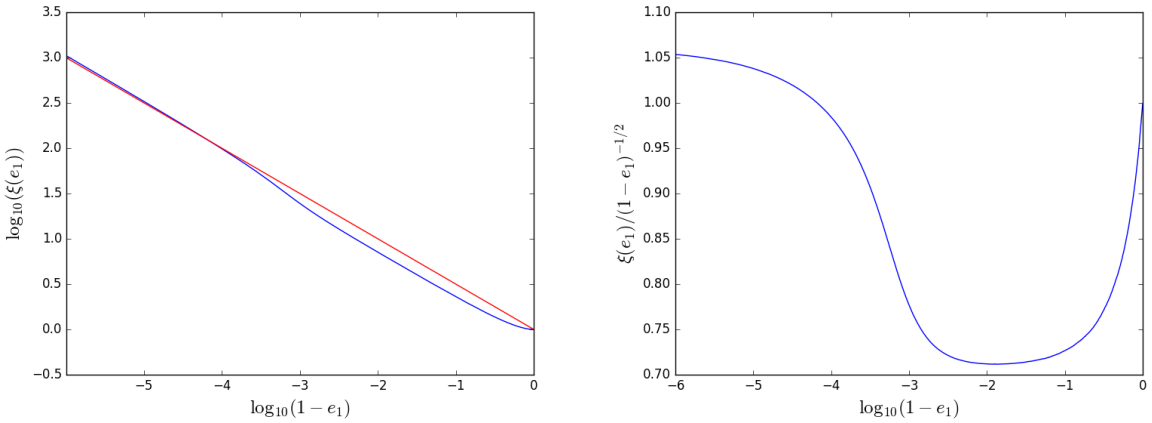


**Figure 3:** (Left): The value of the normalized integral in Equation 19 (blue) as a function of of $\log_{10}(1-e_1)$, with $1/\sqrt{1-e_1}$ (red, see Equation 17) for reference. In a system experiencing KL oscillations, the eccentricity can reach $1-e_1 \sim 10^{-6}$. In this region of parameter space, the integral becomes large enough to significantly affect the mass-loss rate. At high enough $e_1$, the normalized integral can bring the mass-loss rate up by a factor of 1000 or more. (Right): The ratio of the true value of the normalized integral to our approximation. The normalized integral is well approximated to within a factor of 0.7 by the analytic estimate $1/\sqrt{1-e_1}$.

to show how the factor might be analytically approximated to within a factor of two by the approximation derived in Equation 17. By implementing this factor into Equation 15, we arrive at an orbit-averaged model for the mass-loss of an eccentric binary system, which can then be incorporated into the equations from Ford et al. (2000), Blaes et al. (2002), and Michaely & Perets (2014). We call the enhancement factor for the mass-loss of an eccentric binary over a circular binary (here, roughly $(1-e_1)^{-1/2}$) the "eccentric mass-loss factor", or the EMLF. Thus, for a binary in an eccentric orbit, the mass loss rate averaged over an orbit is approximately

$$\dot{m}_e = \dot{m}_c \xi(e_1) \sim \dot{m}_c (1-e_1)^{-1/2}, \tag{20}$$

where $\dot{m}_c$ is the mass-loss rate for a circular orbit (see Equation 15) and $\xi(e_1)$ is the EMLF (see Equation 19).

## 2.4 Timescales

From van den Heuvel & van Paradijs (1988), we find that the timescale associated with the evaporation of a companion star ($m_1/\dot{m}_1$) in a circular orbit is

$$\begin{aligned}\tau_{evap,c} &= \left(\frac{3c^3}{2R_0^6}\right)\left(\frac{2Gm_1^2}{R_1^3}\right)\left(\frac{a_1^2}{16\pi^4 f}\right)\frac{P_{spin}^4}{B^2} \\ &= 1.1\times 10^8 \mathrm{yr}\left(\frac{m_1}{0.2M_\odot}\right)^2\left(\frac{R_1}{0.2R_\odot}\right)^{-3}\left(\frac{a_1}{16R_\odot}\right)^2\left(\frac{P_{spin}}{1.6\mathrm{ms}}\right)^4 f^{-1},\end{aligned} \tag{21}$$

in agreement with our earlier estimation of the mass-loss rate (Equation 15). We refer to this as the evaporation timescale or the ablation timescale of a binary system. As in Equation 15, we have assumed $R_0$ = 10 km and $B = 10^9$ G. It should be noted that this timescale is not entirely accurate and should only be used as an order-of-magnitude estimate. For example, as mass is ablated, $m_1$ decreases, and thus $\tau_{evap}$

decreases. For a non-degenerate MS companion, $R_1 \propto m_1$, so the overall effect is to increase the ablation timescale, whereas for a degenerate companion, $R_1 \propto m_1^{-1/3}$, and the overall effect is to decrease $\tau_{evap}$. In addition, $a_1$ increases as $m_1$ decreases (see Equation 4), implying that Equation 21 should be treated as an order-of-magnitude estimate only.

For an eccentric orbit, we say that $\tau_{evap,e} = m_1/\dot{m}_{1,e}$ is:

$$\tau_{evap,e} = \tau_c \xi(e_1)^{-1} \sim \tau_c \left(1 - e_1\right)^{1/2} \tag{22}$$

where $\tau_c$ is the ablation timescale for a circular orbit (see Equation 21). Because $\tau_{evap} \propto \dot{m}_1^{-1}$ and $\dot{m}_1 \propto \xi(e_1) \sim (1 - e_1)^{-1/2}$, for an eccentric orbit, $\tau_{evap,e} \propto \xi(e_1)^{-1} \sim (1 - e_1)^{1/2}$.

Our derivation of $\xi(e_1)$ (the rate of mass-loss enhancement–also the rate of reduction in the ablation timescale, since $\tau_{evap} \propto \dot{m}^{-1}$) assumes a constant eccentricity. However, the inner binary of a dynamically-active triple system undergoing KL oscillations will have an eccentricity that oscillates from $e_{1,0}$ to $e_{1,max}$ (see Equation 1) on a timescale $\tau_{KL} \gg P_{inner}$. For each period, the inner eccentricity is constant, but over many periods, the eccentricity can oscillate to extreme highs. However, the inner binary does not spend all of its time at high eccentricity (see Figure 1, upper left panel), so we cannot estimate the reduction in the ablation timescale for an eccentric orbit, $\tau/\tau_0$, as $(1 - e_{1,max})^{1/2}$. We wish to find an expression for the reduction in the ablation timescale of an eccentric binary experiencing KL oscillations as a function of $1 - e_{1,max}$. We seek the average EMLF over a KL cycle.

In a similar method to our estimation of the average mass-loss rate over a period for an eccentric orbit, we estimate the average $\xi(e_1)$ over a KL time (see Innanen et al. 1997; Holman et al. 1997). We integrated $\xi(e_1)$ (not our approximation $(1 - e_1)^{-1/2}$, see Figure 3, right panel) for a KL time, dividing by $\tau_{KL}$ to normalize. We present our results in Figure 4.

In Figure 4, we iterated over many initial $\cos(i)$ while keeping $e_{1,init}$ constant at 0.01. Our motivation for considering eccentricity-aided ablation is the long-orbit, eccentric MSP systems. We believe the inner binaries for these systems may have undergone CE evolution, resulting in low initial eccentricities. The average of the EMLF over a Kozai cycle appears to depend on $e_{1,init}$ in a way that is not contained in $e_{1,max}$. Raising the initial eccentricity from 0.01 to 0.5 (see Section 5) appears to considerably increase the average EMLF. For now, we choose to focus on systems that begin with low initial eccentricity; we leave the consideration of initial eccentricity on the Kozai-time averaged EMLF for future works.

As expected, a system's ablation time does not decrease by the estimated factor $(1 - e_1)^{-1/2}$ (given in Equation 17), as appropriate for constant eccentricity, because of the small amount of time the inner binary actually spends at very high eccentricity during the KL oscillations (see Figure 1, upper left panel); our fit from Figure 4 is

$$\langle \xi(e_1) \rangle \approx 0.99 \left(1 - e_{1,max}\right)^{-1/15}. \tag{23}$$

Applying this averaged factor to Equations 21 and 22, we arrive at the true equation for $\tau_{evap}$, averaged over KL cycles:

$$\begin{aligned} \tau_{evap} &= 1.1 \times 10^8 \text{ yr} \left(\frac{m_1}{0.2 M_\odot}\right)^2 \left(\frac{R_1}{0.2 R_\odot}\right)^{-3} \left(\frac{a_1}{16 R_\odot}\right)^2 (1 - e_{1,max})^{1/15} f^{-1} \\ &= 1.0 \times 10^8 \text{ yr} \left(\frac{m_1}{0.2 M_\odot}\right)^2 \left(\frac{R_1}{0.2 R_\odot}\right)^{-3} \left(\frac{a_1}{16 R_\odot}\right)^2 \cos(i)^{2/15} f^{-1}. \end{aligned} \tag{24}$$

In the second expression, we have used Equation 1 to relate $e_{1,max}$ and $\cos(i)$ and assumed that $1 + e_{1,max} \sim 2$.

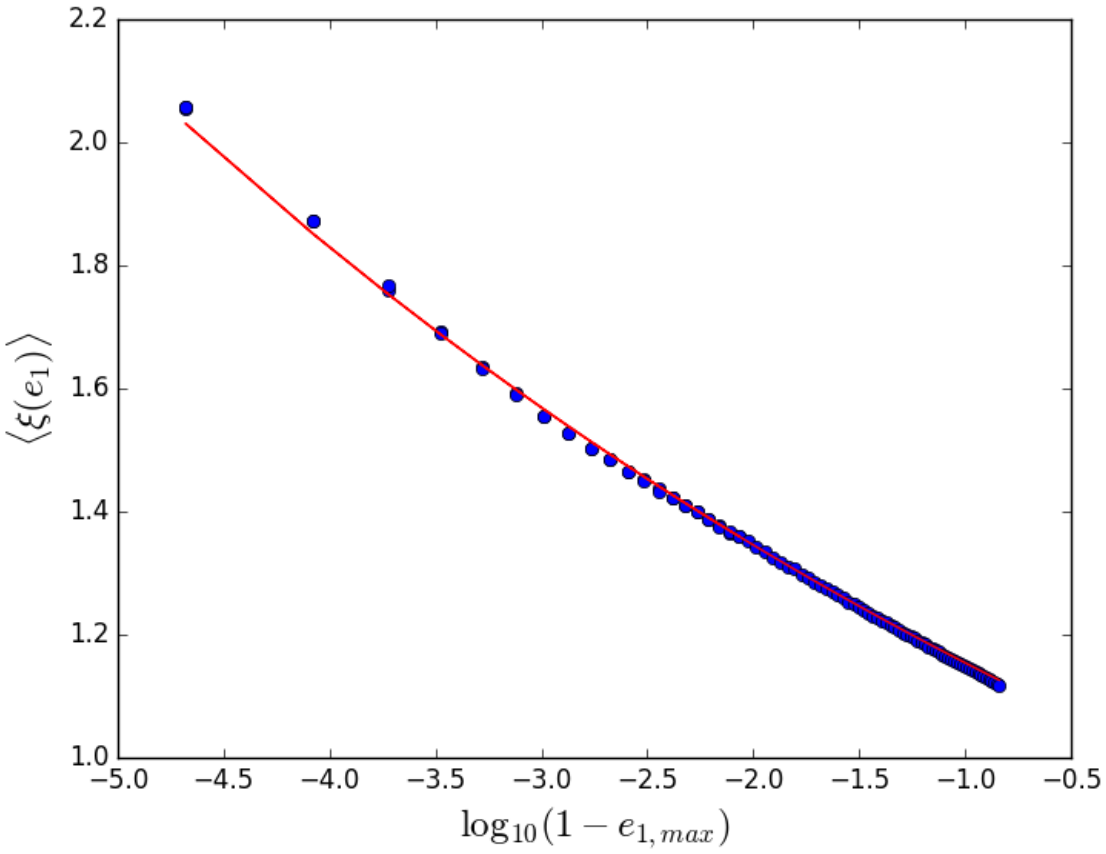


**Figure 4:** The normalized integral of $\xi(e_1)$ over a Kozai-Lidov time. We evaluated the integral over various initial $\cos(i)$, from -0.1 to 0.4 in 100 steps (blue dots). We show the relationship between the EMLF averaged over a Kozai time and $e_{1,max}$, the maximum eccentricity achieved during a single KL oscillation (see Equation 1). We find the data fit the function $\langle \xi(e_1) \rangle = 0.99\,(1 - e_{1,max})^{-1/15}$.

The relationship between eccentricity and the reduction in the ablation timescale is rather weak; for a binary reaching $1 - e_{1,max} \sim 10^{-4}$, the reduction in the ablation timescale is only a factor of 1.85 or so. Systems starting with higher initial eccentricity $e_{1,0}$ will have higher overall average EMLF, as a result of the approximate $(1 - e_1)^{-1/2}$ dependence of $\xi(e_1)$ for constant $e_1$. We discuss this and other future directions for this project in Section 5.

There are two other timescales we consider here as well: the pulsar spindown timescale ($P_{spin}/\dot{P}_{spin}$– e.g., van den Heuvel & van Paradijs 1988) and the gravitational wave (GW) merger timescale (the time required for a binary system to merge via emission of GWs). The timescale associated with a pulsar spinning down ($P/\dot{P}$) is (van den Heuvel & van Paradijs, 1988):

$$\begin{aligned} \tau_{SD} &= \frac{P_{spin}^2}{B^2} \frac{3c^3 I}{8\pi^2 R_0^6} \\ &= 1.1 \times 10^8 \text{ yr} \left( \frac{P_{spin}}{1.6 \text{ ms}} \right)^2 \left( \frac{B}{10^9 \text{ G}} \right)^{-2} \left( \frac{m_0}{1.6 M_\odot} \right) \left( \frac{R_0}{10 \text{ km}} \right)^{-4}, \end{aligned} \tag{25}$$

where we have used the moment of inertia for a sphere of constant density, $I = \frac{2}{5} m_0 R_0^2$. After $\tau_{SD}$, the

pulsar's spin period will have decreased significantly, and $\dot{E}_{NS}^{wind}$ decreases as well.

The GW merger time for a binary system is given by (Peters, 1964):

$$\tau_{GW} = 1.6 \times 10^{13}\text{yr} \left( \frac{2M_\odot^3}{m_0 m_1 (m_0 + m_1)} \right) \left( \frac{a_1}{0.1\text{AU}} \right)^4 (1 - e_1)^{7/2}. \quad (26)$$

Substituting in this relationship between eccentricity and inclination (after accounting for the amount of time the binary actually spends at this high eccentricity), the timescale becomes (Thompson, 2011):

$$\tau_{GW} = 8.7 \times 10^{9}\text{yr} \left( \frac{2M_\odot^3}{m_0 m_1 (m_0 + m_1)} \right) \left( \frac{a_1}{0.1\text{AU}} \right)^4 \left( \frac{\cos i}{0.2} \right)^6, \quad (27)$$

which shows that binaries with a highly inclined triple merge much faster than binaries without. Equation 27 demonstrates that the GW merger timescale is strongly dependent on $a_1$. After the LMXB phase, a MSP and its companion may be close enough to merge in less than a Hubble time, given the assistance of KL-induced eccentricity oscillations. However, this paper focuses on a total ablation outcome, rather than a GW-driven merger. As such, we choose our parameters to generate systems that will not merge before a spindown time, to explore the combined effects of KL oscillations and ablative mass loss.

# 3 General Exploration of Eccentricity-Enhanced Ablation

To determinine the evolution of systems undergoing KL oscillations and ablative mass loss, we integrate the equations found in Ford et al. (2000), Blaes et al. (2002), and Michaely & Perets (2014), as well as those we derive above. We acknowledge that the systems we are considering are tight, and tidal effects may play a role. To account for this, we include the term for periastron precession due to tidal effects $\dot{g}_{1,tide}$ found in Fabrycky & Tremaine (2007) and define a tidal separation, $R_{tide} \equiv 3R_1$. At separations closer than $R_{tide}$, we consider tidal forces to be the dominating effect in the future evolution of the system. In our integration, we approximate the value of $\xi(e_1)$ as this saves us evaluation of the full integral (see Equation 19) or doing a table lookup. Our results from the right panel of Figure 3 indicate that the difference between the analytic approximation $(1 - e_1)^{-1/2}$ and the actual $\xi(e_1)$ may be non-negligible; for $1 - e_1$ from $10^{-1}$ to $10^{-3}$, the error in the analytical approximation is around 25 percent. We approximate the value of $\xi(e_1)$ by adding additional terms in a piecewise function, minimizing our error. Instead of the approximation that the $\xi(e_1) = (1 - e_1)^{-1/2}$, we say that:

$$\dot{m}_1 = \dot{m}_e f(e_1), \quad (28)$$

where $f(e_1)$ is a piecewise function of $e_1$, and $\dot{m}_e$ is our previous model for the mass-loss rate (see Equation 20). The right panel of Figure 3 shows $\xi(e_1)$ for an orbit at eccentricity $e_1$ divided by our analytical estimate $(1 - e_1)^{-1/2}$. To reduce error in our analytical estimate, we model the curve in the right panel of Figure 3 as a piecewise series of lines, functions of $\log_{10}(1 - e_1)$. We then multiply the equations by our earlier analytical estimate (see Equation 17) to arrive at a closer approximation of the real EMLF. We present the curve from the right panel of Figure 3 (blue), as well as our piecewise fit (green), and $\xi(e_1)$ divided by the new analytical estimate (red) in Figure 5. After applying this new approximation, the error in our employed EMLF reduces to mostly less than four percent over the full range of $(1 - e_1)$.

Next, we begin to apply our methods to the problem of long-orbit MSPs. We simulate several NS-MS systems, varying the inner and outer periods to sample the population. We consider a primary NS of mass $m_0 = 1.6M_\odot$, a secondary MS star of mass $m_1 = 0.2M_\odot$, and a tertiary of mass $m_2 = M_\odot$. A primary mass of $1.6M_\odot$ best represents the population we are studying; the systems in Champion et al.

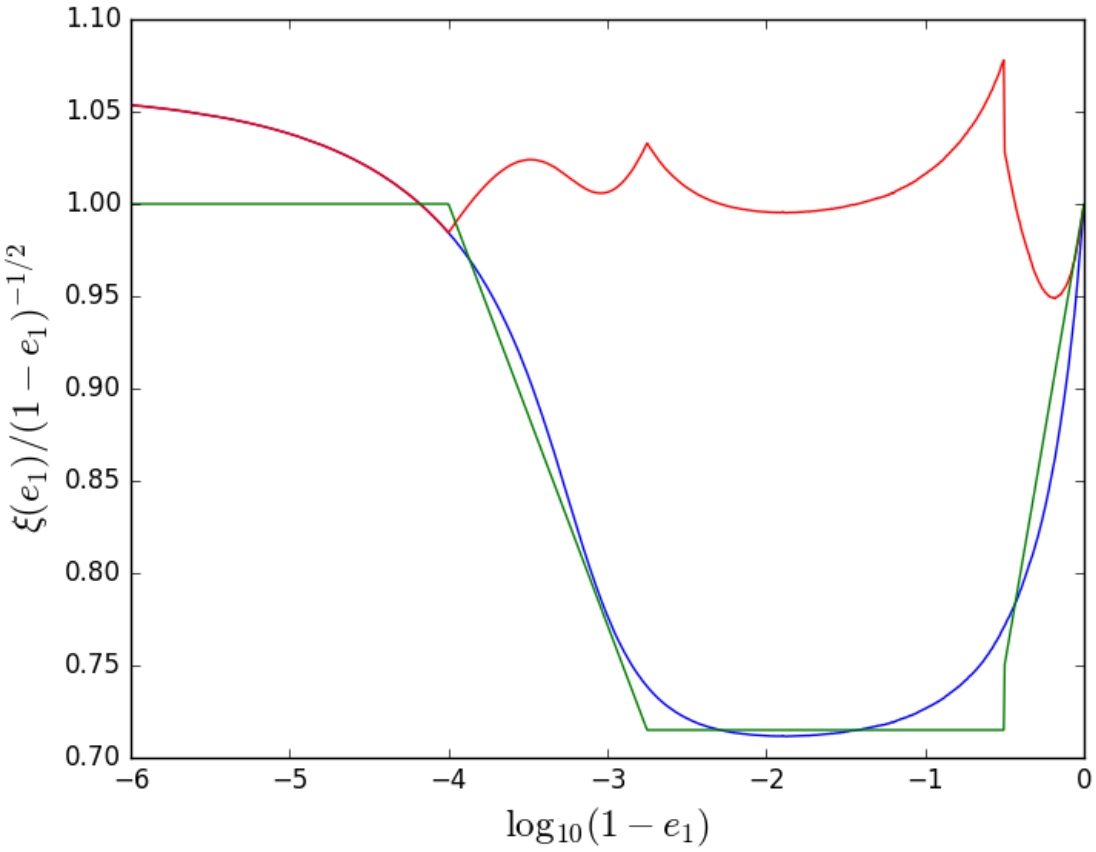


**Figure 5:** The right panel of Figure 3 with further approximations made. The blue curve is the same as in Figure 3. The green lines show our piecewise estimations of the errors made by the first-order analytic approximation (see discussion after Equation 28). The curve in red is $\xi(e_1)$ divided by our analytical estimate after applying our next-order approximations to the analytic expression.

(2008); DeCesar et al. (2015); Antoniadis et al. (2016); Barr et al. (2017); Knispel et al. (2015) have MSPs with masses on average $1.6M_\odot$. We chose initial secondary masses of 0.2 $M_\odot$ because we found this value to be a fair representation of the mass distribution for MSP companions after the LMXB phase (see Özel & Freire (2016) and references therein). Choosing an initial secondary mass greater or less than 0.2 $M_\odot$ would raise or lower the ablation time in a manner generally consistent with Equation 21. A tertiary mass of $M_\odot$ was chosen to represent the system of Champion et al. (2008). In our simulations, we use the mass-radius relation found in van den Heuvel & van Paradijs (1988) for the radius of the secondary:

$$\begin{aligned} R_1/R_\odot &= m_1/M_\odot & m_1 &> 0.075M_\odot \\ R_1/R_\odot &= 0.075M_\odot(m_1/0.075M_\odot)^{-1/3} & m_1 &< 0.075M_\odot. \end{aligned} \tag{29}$$

Using Equation 27, we set the cosine of the inclination of each system so that, given an initial separation, the inner binary would not merge via GW radiation until after the pulsar spins down; in particular, we set $\cos(i)$ such that $\tau_{merge} = \tau_{spindown}$. For the rest of our orbital parameters, we chose $e_1 = 0.01$, $e_2 = 0.15$, $g_1 = 0$, and $g_2 = \pi$, where $g_1$ and $g_2$ represent the arguments of periastron for the inner

and outer binaries, respectively. We show the reduction in the ablation timescale of eccentric binaries for various values of the inner period in Figure 6. The dashed lines show the evolution of the secondary without the presence of a perturbing tertiary, whereas the solid lines show the evolution of the secondary undergoing KL oscillations. In all cases, the systems with eccentricity oscillations modulating mass-loss are ablated more rapidly.

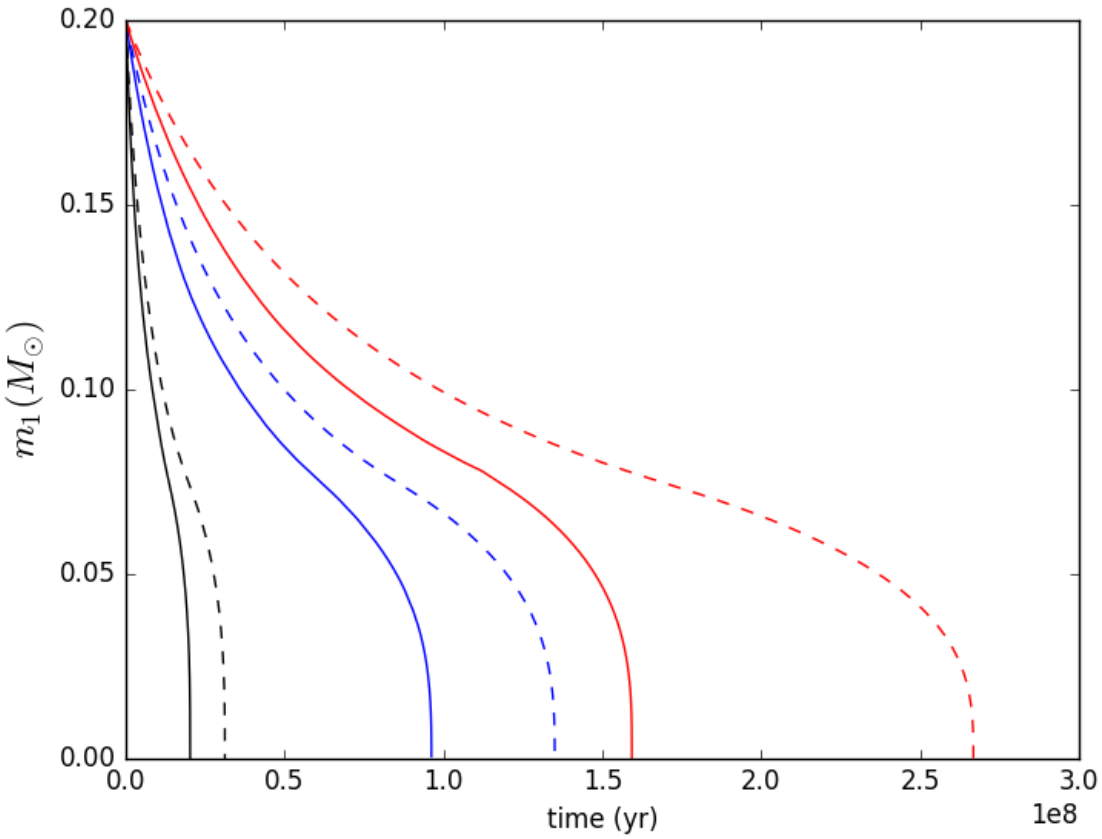


**Figure 6:** We present three systems undergoing ablative mass loss, with (solid) and without (dashed) the presence of a tertiary. The systems have initial inner periods and $\cos(i)$ of 1 day and 0.20 (black), 3 days and 0.125 (blue), and 5 days and 0.10 (red). The initial periods for the outer binaries are 30 days (black) and 50 days (blue, red). The systems begin to accelerate in their ablation as they reach $m_1 = 0.075 M_\odot$. This is a result of the mass-radius relation we used; $0.075 M_\odot$ is when the secondary becomes degenerate.

The eccentricity oscillations induced by the presence of a highly inclined tertiary reduce the ablation times of the systems by a modest factor. For highly inclined tertiaries (see Equation 24) or for higher initial eccentricities (see Section 5), the reduction in the ablation timescale may be significantly larger. In Figure 6, the more inclined systems reach higher $e_{1,max}$, and therefore have their ablation times reduced by a relatively greater amount than those with less inclined tertiaries.

The systems in Figure 6 all begin to turn dramatically as they reach $m_1 = 0.075 M_\odot$. This is due to the degeneracy of the star at this mass. From the mass-radius relationship we used (see Equation 29), at $m_1 = 0.075 M_\odot$, the radius begins to increase as the mass decreases. This effect works to greatly increase $\dot{m}_1$ and reduce $\tau_{evap}$ (see Equations 15 and 21). Because of this sudden increase in mass loss, we considered the possibility of a white dwarf (WD) secondary. The mass-radius relationship of a WD

is similar to that of a degenerate MS star, so the mass-loss rate should accelerate constantly. However, returning to Equation 21, for an average WD ($m_1 = 0.7M_\odot$, $R_1 = R_\oplus$), $\tau_{evap} = 1.4 \times 10^{13}$ yr, and we do not expect this system to ablate, even with the presence of a tertiary. For a less massive WD ($m_1 = 0.2M_\odot$, $R_1 \sim 40R_\oplus$), the ablation timescale is still much larger than the spindown timescale. Substituting a simple mass-radius relationship ($R_1/R_\oplus = (0.7M_\odot/m_1)^{1/3}$) for a WD into Equation 21, we see that, for a circular orbit, it reduces to:

$$\tau_{evap,WD} = 3.85 \times 10^{12} \text{ yr} \left(\frac{m_1}{0.2M_\odot}\right)^3. \tag{30}$$

Here we have left the rest of the parameters from Equation 21 unchanged. We see that as the companion becomes degenerate, the ablation timescale has a cubic dependence on the mass, which can explain the rapid mass loss in Figure 6. We earlier stated that Equation 21 should be used as an order of magnitude estimate, noting its imprecision. Here, we see that, within several orders of magnitude, a WD will likely not be ablated before the pulsar spins down.

The equations we used to evolve these systems are approximated to octupole order, and we believe that any further expansions of the Hamiltonian would not affect the results significantly. The dipole terms (expanding in the limit of small $a_1/a_2$) are exactly zero; the quadrupole terms then are the first nonzero order of the KL-oscillation expansion. As discussed above, the octupole terms are dependent on the mass-difference between the two bodies. The main "selling point" of the hexadecapole terms (see Will 2017) is that they have important effects on equal-mass or near-equal-mass inner binaries, where the octupole order terms have little strength (see Equation 3). In the systems we are evolving, the inner binary has a large difference between the primary and secondary masses. The octupole terms are strong; therefore, the hexadecapole terms will likely have little significance in determining the evolution of these systems.

For a binary this tight, tidal effects can play a role. We define $R_{tide} \equiv 3R_1$ as the critical separation when tidal effects will dominate the evolution of the binary. This will then set an upper bound on the eccentricity, and thus the EMLF. The maximum eccentricity a system can reach is set by the criterion $a_1(1 - e_1) = R_{tide}$; eccentricity greater than this will likely result in tidal damping, significantly decreasing the eccentricity. Thus, the maximum mass-loss factor is approximately $\sqrt{a_1/R_{tide}}$, since $\xi(e_1) \sim (1 - e_1)^{-1/2}$. It is true that a wider binary than those we have considered here will be able to reach higher eccentricities and therefore a higher EMLF. However, the reduction in the ablation time is, at its largest, proportional to $\sqrt{a_1}$, whereas the fraction of material actually striking the secondary is proportional to $a_1^{-2}$. Therefore, the overall relationship between $\tau_{evap}$ and $a_1$ is that $\tau_{evap} \sim a_1^{3/2}$. A wider binary allows higher eccentricities, but will still result in an overall increase in the ablation time.

We discussed earlier in the paper the importance of the mass differential between the primary and secondary (see Equation 3) in driving the inner binaries to higher eccentricities. Because the binaries were so tight, they were restricted in their eccentricity by our tidal criterion, as well as the detuning of KL oscillations by tides (Ford et al., 2000; Blaes et al., 2002). The rate of periastron precession $\dot{g}_{1,tide}$ (Fabrycky & Tremaine, 2007), which we included in our integration determining the evolution of each system, has a very strong dependence on periastron distance; therefore, as the already tight inner binaries approached their maximum eccentricities, tidal effects took over and stunted the growth of $e_1$. The inner binaries in our systems were only able to reach $1 - e_{1,max} \sim 10^{-2}$. The octupole terms, driven by the difference in masses $m_0 - m_1$, drove the binaries to higher eccentricities than the quadrupole terms alone, but the tidal effects acted to reduce the strength of this effect. We leave the question of the relative strength of the quadrupole, octupole, hexadecapole, and further expansion terms for future works.

In Figure 6, we show the secondary masses equaling zero as they finish ablating away. In reality, the mass-radius relationship we chose would not hold beyond a certain point in the secondary's mass loss. What would likely happen is that the radius of the degenerate secondary would increase until some $R_{max}$,

at which point it would then shrink to some final radius, likely the size of a planet. As the radius begins to decrease again, the rate of ablative mass loss decreases accordingly. The companion could reach some final state of a planet-sized object (with a radius so small that $\dot{m}_1$ is negligible), or it could evaporate entirely. The primary could also collide with or tidally shred the secondary. In all of these scenarios, what remains of the secondary is likely not massive enough to indicate that the pulsar is actually in a triple system. We would say at this point that the secondary has been sufficiently ablated and that the primary and tertiary are a long-orbit, eccentric ($e = e_2$) binary system, similar to those recently discovered.

# 4 Tight Triples

The eccentricity-aided ablation effect can reduce the ablation timescales of binaries with highly inclined tertiaries by a modest factor. However, such a triple system would need to be incredibly compact to produce a long-orbit MSP binary like the ones we observe today. In our formation scenario, we propose that, as the inner binary was on the main sequence, there was a tertiary evolving alongside it. To achieve the compactness of the outer binary, triple CE evolution may have occurred, however we neglect it here–see Iben & Tutukov (1999). In this section, we discuss how these compact triples may have formed.

## 4.1 Expansion of Orbits due to Mass-Loss

In its evolution, the inner binary of our proposed original triple system underwent a period of dynamical mass loss when the primary formed a NS. We have assumed that the secondary is a MS star and does not undergo any sort of mass loss to form a compact object. For dynamical mass loss, the initial and final $a$ and $e$ are related by the following (Hills, 1983):

$$a_f/a_0 = \frac{M_0 - \Delta M}{M_0 - (2a_0/r)\Delta M} \tag{31}$$

$$e_f = \left(1 - (1 - e_0^2)\left(\frac{1 - (2a_0/r)(\Delta M/M_0)}{(1 - \Delta M/M_0)^2}\right)\right)^{1/2} \tag{32}$$

where $r$ is the binary's position in its orbit at the time of the SN and $M_0$ is the total mass in the binary before the SN. We see that if $\Delta M > M_0(r/2a_0)$, the system will become unbound. The inner binary will likely have undergone several CE phases, circularizing the orbit. Thus, $r \sim a_1$, so if more than half the total mass is lost in the SN, the inner binary will become unbound.

In the same way, the outer binary also increases in size due to the dynamical mass loss. However, because $M_0$ increases for the outer binary while $\Delta M$ remains constant, it is more likely for the outer binary to remain bound than the inner binary. We know that tight (inner) binaries exist and continue on to form MSPs, so for these systems, any tertiary should also remain bound.

If some sort of triple CE evolution took place, the SN would impart the outer orbit with some eccentricity after it had been circularized, leading to the eccentric binary we observe today.

## 4.2 Binary Stellar Evolution

We evolved around $10^8$ binary systems using a Binary Stellar Evolution (BSE) code (Hurley et al., 2000, 2002) that would eventually result in a NS primary and a WD secondary, recording the masses, separations, and eccentricities of the binaries before and after each mass-loss episode. After evolution, roughly $4 \times 10^6$ systems survived. The initial binary separation was equally distributed in the log between 1 and $10^6 R_\odot$; the eccentricity was randomly drawn from 0 to 1; the primary mass was chosen randomly according to a

Salpeter mass function (see Salpeter 1955); the secondary mass was drawn randomly from 0.1 $M_\odot$ to the mass of the primary.

We inserted triples with random initial orbital parameters into the systems that remained bound throughout the binary evolution. $m_2$ was equally distributed between 0 and $m_0$; $g_1$ and $g_2$ (arguments of periastron) were equally distributed in the range from 0 to $2\pi$; the cosine of the relative inclination between the inner and outer binaries was equally distributed from -1 to 1; $a_2$ was equally distributed in the log between $3a_1$ and $30a_1$; $e_2$ was drawn by taking the square root of random number between 0 and 1. Each surviving binary was injected with a triple ten different times.

After the initial parameters were drawn, we evolved $a_2$ and $e_2$ under Equations 31, 32, and 4 (assuming $e_f = e_0$ during adiabatic mass-loss) for the mass-loss episodes of the NS primary and the WD secondary to simulate a triple evolving alongside the binary. Looking at these final values, we sought a system with a small enough $a_1$ and $a_2$ that it could ablate away with the help of the EMLF. We present the results of our triple-injection in Figure 8, as well as our original sample of binaries in Figure 7.

The upper left panel of Figure 7 shows our distribution of primary masses $m_0$. Most begin with $m_0$ between 6 and 11 $M_\odot$. After evolution, there is a strong peak in primary masses at 1.4 $M_\odot$, the mass of most newly-born NSs. The lower left panel displays our distribution of binary separations. The lower right panel shows the initial and final distributions of eccentricity. Nearly all of our binary systems went through some form of CE evolution; this dramatically damps the eccentricity, resulting in the sharply peaked final distribution.

The upper right panel of Figure 8 shows that, in accordance with Equation 5, the orbit of the outer binary expanded as mass was lost. Because we assumed a distant tertiary, we ignored any possible interactions between the tertiary and the inner binary. Without considering triple CE evolution, the outer orbit only expanded, and we failed to find any systems that remained bound with $a_2 < 1$ AU. We believe this does not preclude a tight triple as the origin of these relatively isolated MSPs. It is probable that with a compact system, the tertiary may have entered the envelope of the primary – supergiants have envelopes AUs wide. This would shrink the outer semimajor axis considerably and perhaps bring the orbit close enough to generate the tight triple system required for a long-orbit MSP to be produced. The outer orbit need not be circularized for this to have occurred; the SN of the primary would have been able to endow the outer orbit with eccentricity (see Equation 32).

# 5 Further Studies

This paper was designed to investigate the efficacy of eccentricity-aided ablation in removing the companions of MSPs. We have shown that binaries excited to high eccentricities will ablate their companions by a modest factor faster than circular binaries. This paper is not exhaustive, however, and we leave some options open for future investigations.

We derived an expression for the dependence of the EMLF, averaged over a Kozai time, on the maximum eccentricity of the binary. We considered this in the limit of low eccentricity systems ($e_{1,init} = 0.01$), as this is likely the case for a tight MSP binary having undergone CE evolution and mass transfer after NS formation. However, the Kozai-time averaged EMLF appears to have a modest dependence on initial eccentricity–raising $e_{1,init}$ from 0.01 to 0.5 increased the EMLF by roughly a factor of two (see Figure 9). In this paper, we study systems with low initial eccentricity, but a full study of the EMLF should not ignore its dependence on $e_{1,init}$. To demonstrate the effects of changing $e_{1,0}$, we present the average EMLF (discussed in Section 2.4) as a function of $e_{1,max}$ for $e_{1,0} = 0.5$, up from 0.1, in Figure 9 (blue dots). The line in red is our approximation from Figure 4 (see Equation 23).

We referenced but did not explore the concept of triple CE evolution. We hypothesized that this may have shrunk the outer orbit of the tertiary enough to ablate away the secondary and result in what we

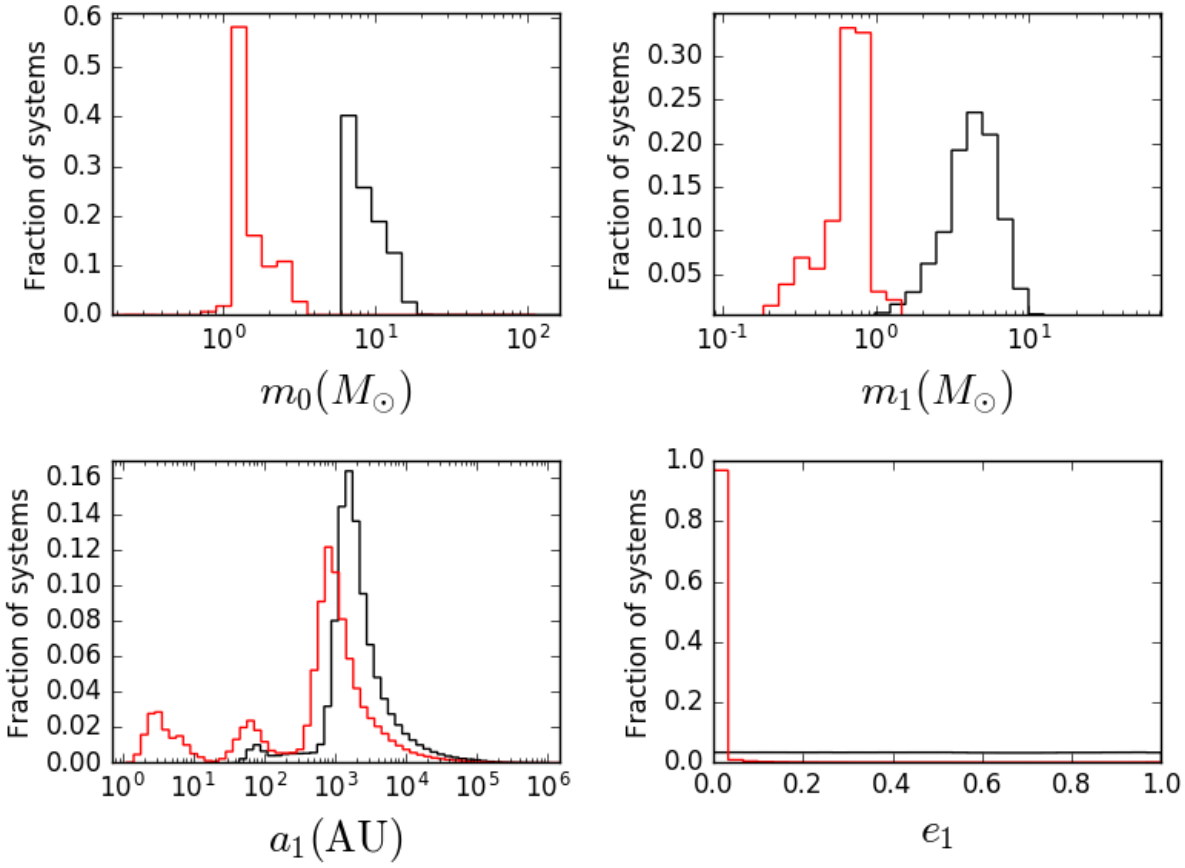


**Figure 7:** We present the results from our BSE code. We generated around $10^8$ original systems which, after evolution, left around $4 \times 10^6$ systems that remained bound and did not merge, forming NS-WD binaries. We present those four million systems here, showing the masses of the primary and secondary, as well as the semimajor axis and eccentricity of the systems. We show the values before (black) and after (red) BSE.

observe today, but we did not investigate triple CE evolution. We leave this unexplored for future papers, and we refer the reader to Iben & Tutukov (1999), the only major publication discussing the subject, as of the publication of this paper.

We leave the topic of tides largely unexplored. From Fabrycky & Tremaine (2007), we see that $\dot{g}_{1,tide} \propto (a_1(1-e_1^2))^{-5}$, so for sufficiently small and eccentric orbits, tidal interactions will detune KL oscillations. We define a critical radius $R_{tide}$ (Section 3) where we believe tidal interactions will begin to dominate and use this to set an upper limit on the EMLF. There is a regime of systems that will merge due to the influence of the tertiary. These systems evolve as the ones discussed in this work; however, these systems have more highly inclined tertiaries than those in this work. As a result, the systems reach higher eccentricity and are more likely to reach $a_1(1-e_1) = R_{tide}$. The GW merger timescale of these systems then becomes relatively short, and the system merges, leaving the product of the merger and the former tertiary as a long-orbit, eccentric MSP binary. This is a formation method for the recent class of eccentric MSP binaries that we did not consider, as this work is focused largely on ablation. Future works may wish to investigate this as an alternative origin channel for the class of long-orbit, eccentric MSP binaries.

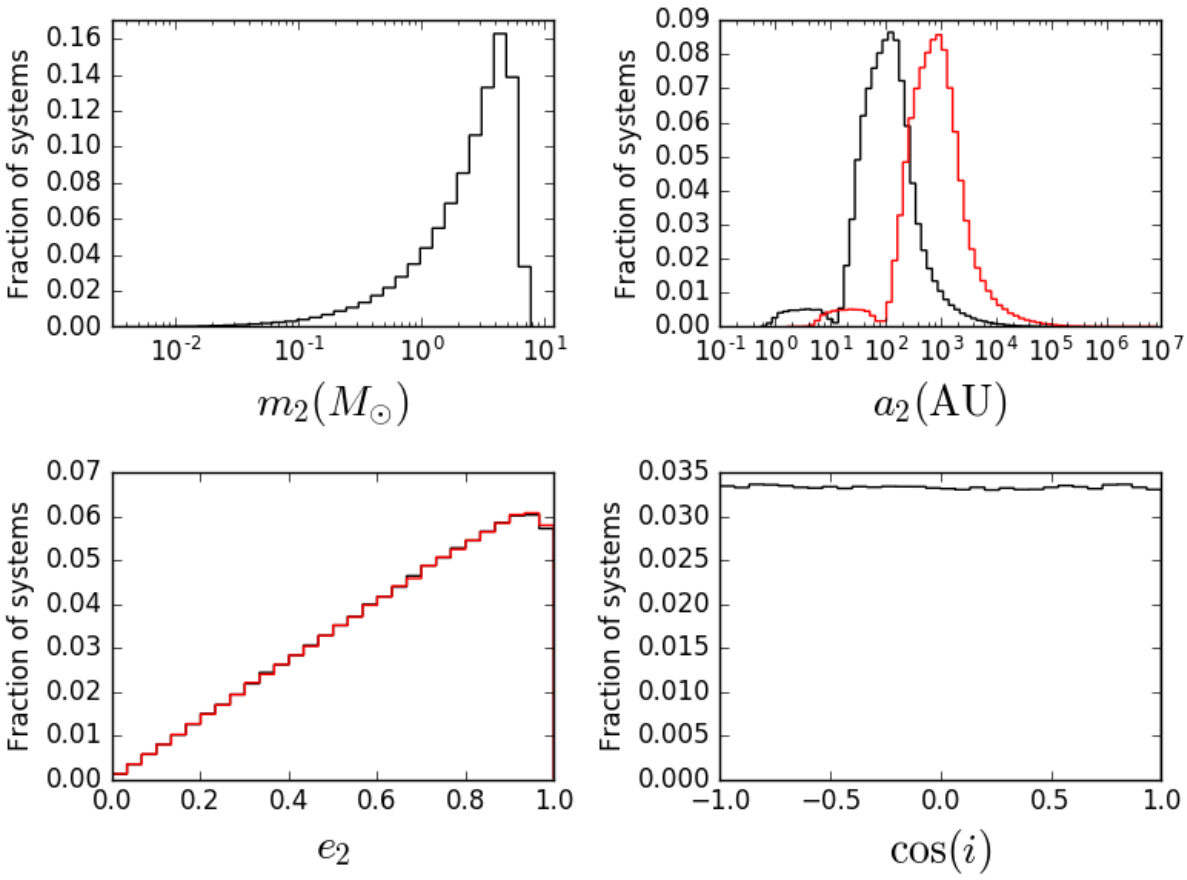


**Figure 8:** The orbital elements of the binary systems from Figure 7 after tehy have been injected with triples, 10 randomly drawn per binary system. The systems with triples that remain stable and do not merge are shown here, with their their mass, semimajor axis, eccentricity, and $\cos(i)$ distributions shown here. We show the values before (black) and after (red) the systems evolved due to mass loss of the primary and secondary.

## 6 Discussion

The presence of a relatively distant companion star as well as a non-zero eccentricity in the observed binary of the recently discovered class of long-orbit, eccentric MSP binaries indicates that the observed companion is not the one that recycled the MSP. One possibility is that this indicates the presence of a triple companion and that the tertiary is what we observe today.

We showed that, averaging over an orbit, eccentric systems have greater ablative mass loss rates than circular systems do (see Figures 3 and 4, as well as Equation 20). We demonstrated how KL-active systems use this to decrease the ablation time of the inner binary of a triple system by a modest factor (see Figure 6 and Equation 24). This then increases the parameter space of systems that ablate before their spindown time, bringing systems that otherwise would not ablate much at all into the realm of possible isolated MSP progenitors. Because the inner binaries do not spend all of their time at high eccentricity, a second timescale-averaging was needed. We derived an approximate expression for the true eccentric mass-loss rate, averaged first over a period, which we call the EMLF, then over a Kozai time. We find that the timescale for ablation is reduced by a factor of roughly $(1 - e_{1,max})^{1/15}$ (see Figure 4), where $e_{max}$ is the maximum eccentricity a system reaches in a single KL cycle (see Equation 1). This translates to a

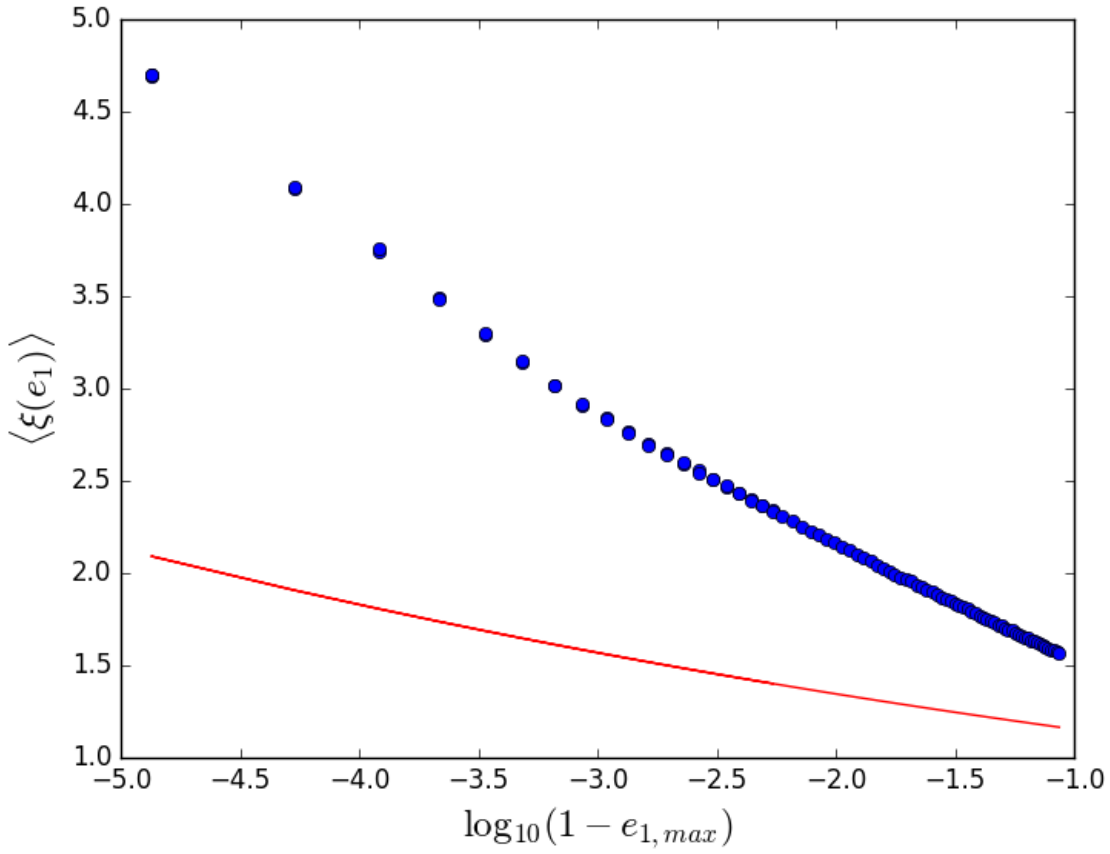


**Figure 9:** The average EMLF (discussed in Section 2.4) as a function of $e_{max}$ for $e_{1,0} = 0.5$ (blue dots). We show for reference the fit used in Figure 4 (red line; $\langle \xi(e_1) \rangle = 0.99 \left(1 - e_{1,max}\right)^{-1/15}$) to demonstrate the effects of changing $e_{1,0}$.

reduction factor of $\cos(i)^{2/15}$, where $i$ is the initial mutual inclination bewteen the inner binary and outer binary. The average of the EMLF over a Kozai time appears to depend on the inital $e_1$ in a manner not contained in $e_{1,max}$. We choose to focus on systems with low initial $e_1$ (after having gone through CE evolution). We consider the effects of this ablative mass loss on planetary systems in Appendix A.

We were unable to find a system in our binary sample that produced a tight enough triple to ablate away (see Figure 8); we believe that this is evidence for triple CE evolution having occurred. We "injected" triples into binary systems, and in our subsequent evolution assumed no interactions between the tertiary and the inner binary. This is likely a flawed assumption, as a red supergiant has a massive envelope at its maximum, and would likely envelop a tertiary at AU separation. This triple CE evolution may produce a tight enough triple system to excite the inner binary to sufficiently high eccentricities, driving the system to ablate away in less than a spindown time, resulting in what we see today. Such a system would begin as a stable triple system. As the primary evolves off the main sequence, its outer envelope expands, swallowing the secondary and even the tertiary. This shrinks the inner and outer binary orbits dramatically, producing a tight triple system, which then undergoes KL oscillations and perhaps ablate the secondary away. The stability of the system during the triple CE evolution is uncertain, and as this paper is only focused on triple CE evolution as means to an end, we reference the idea, but leave it largely unexplored for future works.

## Acknowledgments

This work is supported in part by NSF Grant 1313252. AJT thanks Dr. Todd Thompson for his ideas, his support, and his time. This project surely could not have been completed without his guidance. AJT also thanks Tim Linden for running a suite of BSE models. AJT thanks Xiao Fang and Joe Antognini for their enlightening discussions. AJT finally thanks the SURP program at the Ohio State University for its support in this project.

## A Planetary Migration

In part because of the selection effects of radial velocity exoplanet surveys, many large-mass planets have been discovered orbiting their host stars at less than AU separation. A leading hypothesis for the formation of these "hot Jupiters" involves KL oscillations (see Papaloizou et al. 2007 and references therein). The hypothesis is that these Jupiter-mass planets form at AU separation, become driven to high eccentricities by a highly inclined tertiary, and tidal forces migrate the planets inward.

These systems are undergoing mass loss as well; we refer the reader to Murray-Clay et al. (2009) for a thorough discussion of planetary mass loss. As we have demonstrated in this paper, systems undergoing periods of high eccentricity will experience greater mass loss. In our scenario, the rate of mass loss was proportional to the inverse square of the separation–by averaging the separation over an eccentric orbit, we arrived at the EMLF (see Section 2.3).

From Murray-Clay et al. (2009), the rate of mass loss depends on the UV flux of the host star. For low UV flux stars, $\dot{M} \propto F_{UV}^{0.9} \propto a_1^{-1.8}$, and for high UV flux stars, $\dot{M} \propto F_{UV}^{0.6} \propto a_1^{-1.2}$. We present the normalized integrals over a period (see Equation 19) of $r^{-1.2}$ and $r^{-1.8}$, as in the left panel of Figure 3, with $r^{-2}$ shown for comparison, in Figure 10.

We have demonstrated that systems undergoing eccentricity oscillations can have their evaporation times reduced by a modest factor (see Equation 24). As we discussed in Section 3, an increase in semi-major axis $a_1$ allows systems to reach greater eccentricity, though it still increases the overall evaporation timescale. As a result, the EMLF can decrease the ablation timescale by a factor of two or so, but not orders of magnitude. We now consider hot Jupiter systems. These systems begin at AU separations and, via KL oscillations, migrate inward in their orbits. Murray-Clay et al. (2009) detail the magnitude of the photoionization heating-induced mass loss on hot Jupiter systems. They find that these systems lose roughly 0.6 percent of their total mass during their host star's MS lifetime. We conclude that the EMLF is not enough to coerce these systems into evaporating a significant portion of their mass as they undergo eccentric migration in their orbits.

## References

Alpar M. A., Cheng A. F., Ruderman M. A., Shaham J., 1982, , 300, 728

Antoniadis J., Kaplan D. L., Stovall K., Freire P. C. C., Deneva J. S., Koester D., Jenet F., Martinez J. G., 2016, , 830, 36

Antonini F., Toonen S., Hamers A. S., 2017, , 841, 77

Barr E. D., Freire P. C. C., Kramer M., Champion D. J., Berezina M., Bassa C. G., Lyne A. G., Stappers B. W., 2017, , 465, 1711

Blaes O., Lee M. H., Socrates A., 2002, , 578, 775

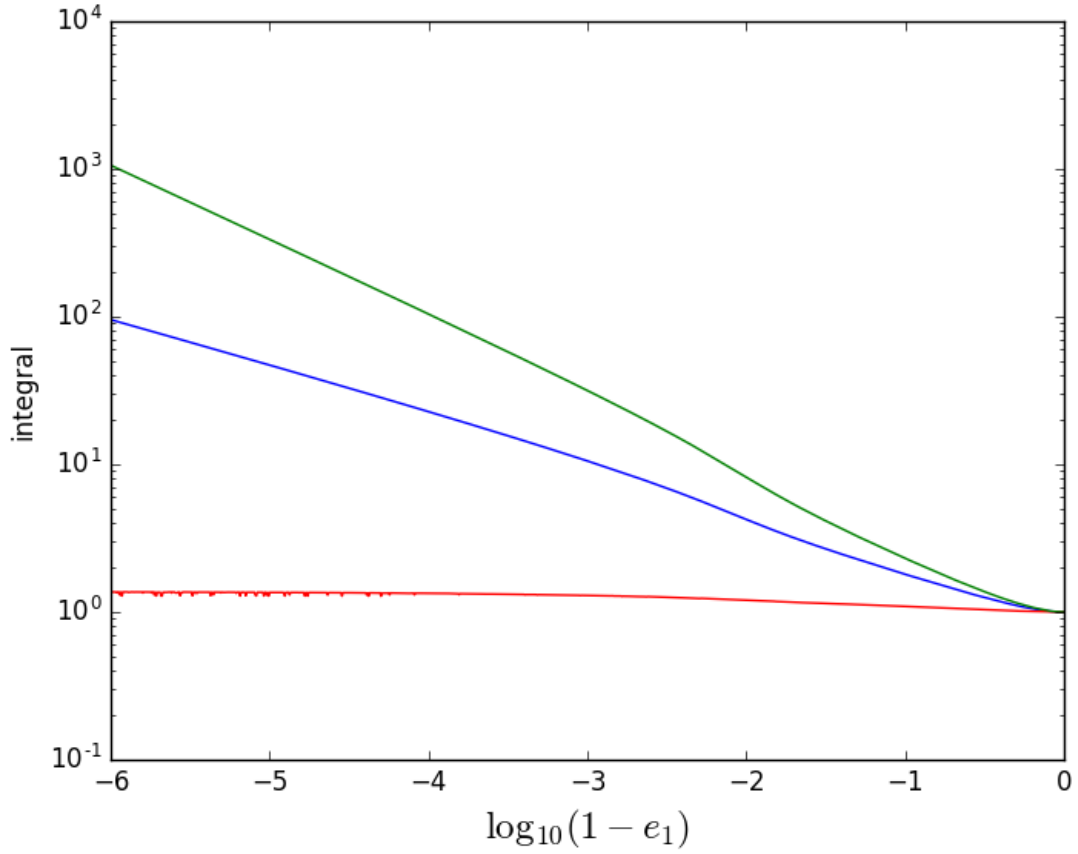


**Figure 10:** The normalized integral of the separation between two bodies in a binary orbit for various power relations (see Equation 19). We show the integral over $r^{-1.2}$ (red), $r^{-1.6}$, and $r^{-2}$ (green, as in Figure 3).


Cash J. R., Karp A. H., 1990, ACM Trans. Math. Softw., 16, 201

Champion D. J., et al., 2008, Science, 320, 1309

DeCesar M. E., Ransom S. M., Kaplan D. L., Ray P. S., Geller A. M., 2015, , 807, L23

Fabrycky D., Tremaine S., 2007, , 669, 1298

Ford E. B., Kozinsky B., Rasio F. A., 2000, , 535, 385

Freire P. C. C., et al., 2011, , 412, 2763

Hills J. G., 1983, , 267, 322

Holman M., Touma J., Tremaine S., 1997, , 386, 254

Hurley J. R., Pols O. R., Tout C. A., 2000, , 315, 543

Hurley J. R., Tout C. A., Pols O. R., 2002, , 329, 897

Iben Jr. I., Tutukov A. V., 1999, , 511, 324

Innanen K. A., Zheng J. Q., Mikkola S., Valtonen M. J., 1997, , 113, 1915

Katz B., Dong S., Malhotra R., 2011, Physical Review Letters, 107, 181101

King A. R., Davies M. B., Beer M. E., 2003, , 345, 678

Knispel B., et al., 2015, , 806, 140

Kozai Y., 1962, , 67, 591

Lidov M. L., 1962, , 9, 719

Lithwick Y., Naoz S., 2011, , 742, 94

Mazeh T., Shaham J., 1979, , 77, 145

Michaely E., Perets H. B., 2014, , 794, 122

Miller M. C., Hamilton D. P., 2002, , 576, 894

Murray-Clay R. A., Chiang E. I., Murray N., 2009, , 693, 23

Naoz S., Farr W. M., Lithwick Y., Rasio F. A., Teyssandier J., 2013, , 431, 2155

Özel F., Freire P., 2016, , 54, 401

Papaloizou J. C. B., Nelson R. P., Kley W., Masset F. S., Artymowicz P., 2007, Protostars and Planets V, pp 655–668

Peters P. C., 1964, Physical Review, 136, 1224

Phinney E. S., Evans C. R., Blandford R. D., Kulkarni S. R., 1988, , 333, 832

Pijloo J. T., Caputo D. P., Portegies Zwart S. F., 2012, , 424, 2914

Salpeter E. E., 1955, , 121, 161

Shappee B. J., Thompson T. A., 2013, , 766, 64

Silsbee K., Tremaine S., 2017, , 836, 39

Thompson T. A., 2011, , 741, 82

Wen L., 2003, , 598, 419

Will C. M., 2017, preprint, (arXiv:1705.03962)

Wu Y., Murray N., 2003, , 589, 605

van den Heuvel E. P. J., van Paradijs J., 1988, , 334, 227